Selective Nucleophilic Attack of Trisulfides. An ab Initio Study

Debbie C. Mulhearn and Steven M. Bachrach*

Contribution from the Department of Chemistry, Northern Illinois University, DeKalb, Illinois 60115

Received June 14, 1996[⊗]

Abstract: The nucleophilic substitution reactions of three trisulfides by thiolate were evaluated at MP2(full)/6-31+G* and MP4SDTQ(fc)/6-311+G**//MP2(full)/6-31+G*. The results show that the gas-phase mechanism at MP2/6-31+G* is addition−elimination. Kinetically, there is a 2−5 kcal mol^{-1} preference for attack at a terminal sulfur over a central sulfur in the same trisulfide. This preference for the terminal sulfur is due to more steric hindrance encountered when the nucleophile attacks the central sulfur versus attacking a terminal sulfur. Hydrogen bonding between the nucleophile and the trisulfide also assists in directing attack to the terminal position. Attack at the terminal sulfur is also thermodynamically favored, a result of the thiosulfenate being a better leaving group than the thiolate. These results provide theoretical support to the findings of Myers et al. that the trigger mechanism for activation of calichaemicin and related enediyne antitumor agents occurs by a multistep process, with a displacement at the terminal sulfur of the trisulfide followed by nucleophilic substitution of a disulfide.

The 1980s were witness to the development of a new class of anticancer agents—the enediynes.[1] These compounds are remarkable for a number of important reasons: they are extremely potent antitumor agents[2] and their chemical structures possess the unusual structural feature of a cyclic enediyne moiety. Calicheamicin (**1**) has garnered much interest over the past decade as chemists have uncovered its exquisite mechanism for physiological activity.[3−11] This stable compound possesses three distinct structural features that are responsible for its mode of action: (1) an enediyne unit, which when activated undergoes Bergman cyclization[12] to give a diradical that cleaves DNA; (2) an oligosaccharide unit, believed to be responsible for the site-specificity[5,13] of calicheamicin by binding to the minor groove of the DNA;[14] and (3) the trisulfide moiety that, upon cleavage, begins the chain of reactions that lead to the Bergman cyclization and subsequent DNA cleavage.

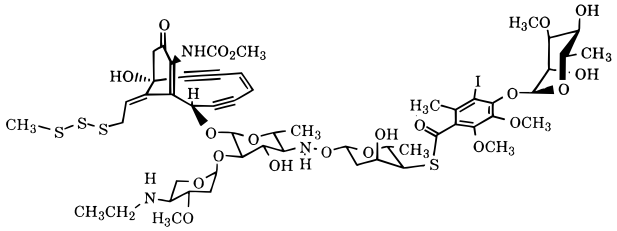

1

The trigger step, the cleavage of the trisulfide by a nucleophilic thiol, is the rate limiting step for the DNA cleavage sequence, at least 50 times slower than the Bergman cyclization.[8] Evans and Seville[15] noted that, in the reaction of thiol with a symmetrical trisulfide, attack at the terminal sulfur is kinetically preferred over attack at the central sulfur. Harpp[16] has noted that desulfurization of trisulfides by phosphines is a two-step process with attack at the terminal sulfur favored over that at the central sulfur. The simplest reaction scheme for the activation of **1** and the related esperamicins has nucleophilic attack at the central sulfur.[1] However, numerous studies have indicated that thiols attack all three sulfurs of **1**, with a preference for attack at the terminal sulfur.[6,8,10] In the most detailed study of the activation of **1**, Myers[10] has detected all four possible cleavage products of **1** by glutathione (see Scheme 1), giving both di- and trisulfide products, all of which show the ability to cleave DNA. Myers demonstrated that the disulfide products from trisulfide cleavage undergo further substitution reactions to produce a common intermediate that cleaves DNA.

We report here ab initio calculations to examine the gas-phase substitution reactions of various trisulfides with a thiolate nucleophile. Our primary interests are in finding if there is any selectivity for attack at either the central or terminal sulfur of a trisulfide compound, both kinetically and thermodynamically, in addition to determining the mechanism. The mechanism for nucleophilic substitution at the sulfur to date is thought to be

[⊗] Abstract published in *Advance ACS Abstracts,* September 15, 1996.

(1) Nicolaou, K. C.; Dai, W.-M. *Angew. Chem., Int. Ed. Engl.* **1991**, *30*, 1387−1416.
(2) Lee, M. D.; Manning, J. K.; Williams, D. R.; Kuck, N.; Testa, R. T.; Borders, D. B. *J. Antibiot.* **1989**, *42*, 1070−1087.
(3) Lee, M. D.; Dunne, T. S.; Siegel, M. M.; Chang, C. C.; Morton, G. O.; Borders, D. B. *J. Am. Chem. Soc.* **1987**, *109*, 3464−3466.
(4) Lee, M. D.; Dunne, T. S.; Chang, C. C.; Ellestad, G. A.; Siegel, M. M.; Morton, G. O.; McGahren, W. J.; Borders, D. B. *J. Am. Chem. Soc.* **1987**, *109*, 3466−3468.
(5) Zein, N.; Sinha, A. M.; McGahren, W. J.; Ellestad, G. A. *Science* **1988**, *240*, 1198−1201.
(6) Ellestad, G. A.; Hamann, P. R.; Zein, N.; Morton, G. O.; Siegel, M. M.; Pastel, M.; Borders, D. B.; McGahren, W. J. *Tetrahedron Lett.* **1989**, *30*, 3033−3036.
(7) DeVoss, J. J.; Hangeland, J. J.; Townsend, C. A. *J. Am. Chem. Soc.* **1990**, *112*, 4554−4556.
(8) Cramer, K. D.; Townsend, C. A. *Tetrahedron Lett.* **1991**, *32*, 4635−4638.
(9) Lee, M. D.; Ellestad, G. A.; Borders, D. B. *Acc. Chem. Res.* **1991**, *24*, 235−243.
(10) Myers, A. G.; Cohen, S. B.; Kwon, B. M. *J. Am. Chem. Soc.* **1994**, *116*, 1255−1271.
(11) Chatterjee, M.; Smith, P. J.; Townsend, C. A. *J. Am. Chem. Soc.* **1996**, *118*, 1938−1948.
(12) Jones, R. R.; Bergman, R. G. *J. Am. Chem. Soc.* **1972**, *94*, 660−661.
(13) Zein, N.; Poncin, M.; Nilakantan, R.; Ellestad, G. A. *Science* **1989**, *244*, 697−699.
(14) Nicolaou, K. C.; Smith, B. M.; Ajito, K.; Komatsu, H.; Gomez-Paloma, L.; Tor, Y. *J. Am. Chem. Soc.* **1996**, *118*, 2303−2304.
(15) Evans, M. B.; Seville, B. *Proc. Chem. Soc.* **1962**, 18.
(16) Harpp, D. N.; Smith, R. A. *J. Am. Chem. Soc.* **1982**, *104*, 6045−6053.

S0002-7863(96)02009-4 CCC: $12.00

Scheme 1

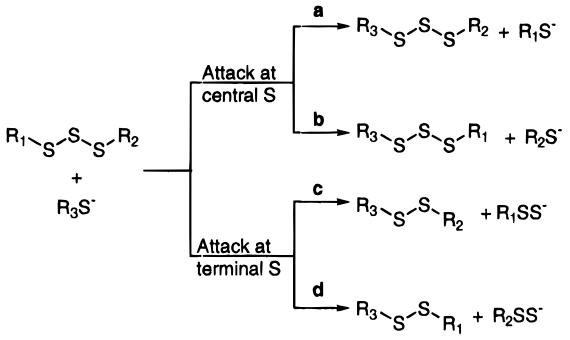

S_N2 in solution, but we[17] have suggested that the gas-phase substitution at a sulfur in disulfides proceeds via an addition−elimination mechanism.

We examine here three sets of reactions which have a thiolate nucleophilic attacking a symmetric (reactions 1 and 2) or unsymmetric trisulfide (reaction 3). These reactions are shown in Scheme 2, where a−d refers to the pathway shown in Scheme

Scheme 2

$$HS^- + HSSSH \rightarrow HSSSH + HS^- \quad \textbf{(1a)}$$

$$HS^- + HSSSH \rightarrow HSSH + HSS^- \quad \textbf{(1c)}$$

$$HS^- + CH_3SSSCH_3 \rightarrow HSSSCH_3 + CH_3S^- \quad \textbf{(2a)}$$

$$HS^- + CH_3SSSCH_3 \rightarrow HSSCH_3 + CH_3SS^- \quad \textbf{(2c)}$$

$$HS^- + HSSSCH_3 \rightarrow HSSSH + CH_3S^- \quad \textbf{(3a)}$$

$$HS^- + HSSSCH_3 \rightarrow HSSSCH_3 + HS^- \quad \textbf{(3b)}$$

$$HS^- + HSSSCH_3 \rightarrow HSSCH_3 + HSS^- \quad \textbf{(3c)}$$

$$HS^- + HSSSCH_3 \rightarrow HSSH + CH_3SS^- \quad \textbf{(3d)}$$

1. From these studies we hope to provide detailed structural and thermodynamic information on the nucleophilic substitution of trisulfides with thiolate which can shed further light on this trigger mechanism.

Computational Methods

Geometry optimizations (along with calculation of analytical frequencies) for all of the species in reactions 1−3 were initially performed at HF/6-31+G*. The HF/6-31+G* TSs for reactions 1−3 and a representative reaction coordinate are shown in Figures 1 and 2. Due to the important role electron correlation plays for reactions at sulfur[17] in defining the reaction coordinate, and hence the mechanism, all species were then fully reoptimized at MP2(full)/6-31+G*. Analytical frequencies were also done at this level to properly characterize each structure and to obtain ZPEs which are scaled by 0.9646.[18] As a verification of the MP2 surface, MP4SDTQ(fc)/6-311+G**//MP2(full)/6-31+G* single point energy calculations were run for the two smallest systems, **1** and **3**. The MP2(full)/6-31+G* geometries for reactions **1a**−**3d** are drawn in Figures 3−5. Optimization of the geometries of **1a-ID1/1c-ID1** and **3d-ID1** at MP2/6-31+G* resulted in a complex where the hydrogen from the trisulfide was transferred to the nucleophile. Therefore, the HF/6-31+G* geometries were used and single point energies at MP2/6-31+G* were run for these complexes. A

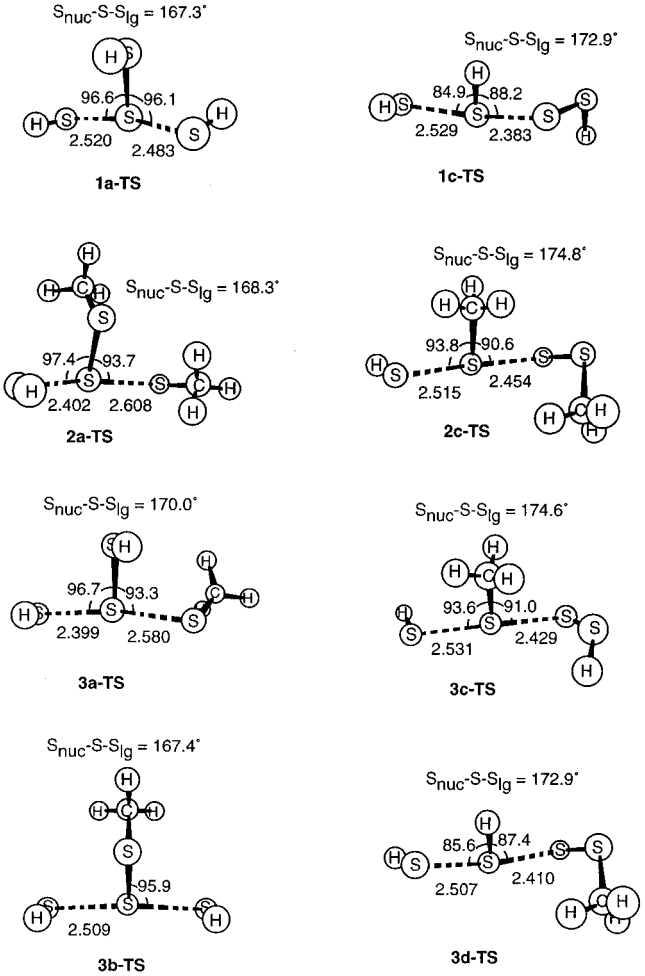

Figure 1. HF/6-31+G* optimized geometries of the TSs for reactions 1−3.

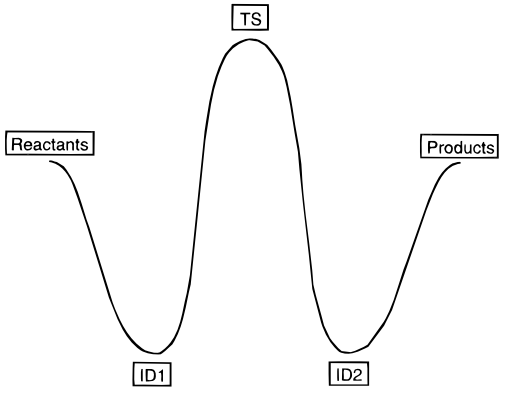

Figure 2. Representative reaction surface for the substitution reaction calculated at HF.

representative reaction coordinate at the MP2/6-31+G* level is drawn in Figure 6. The HF energies for reaction 1−3 are listed in Table 1, and MP2 and MP4SDTQ energies are listed in Table 2. All calculations were performed with GAUSSIAN-92[19] or GAUSSIAN-94.[20]

Results

Comparison of the Mechanism of Reaction 1 at HF and MP2. In our examination of nucleophilic displacement by

(17) Bachrach, S. M.; Mulhearn, D. C. *J. Phys. Chem.* **1996**, *100*, 3535−3540.

(18) Pople, J. A.; Scott, A. P.; Wong, M. W.; Radom, L. *Isr. J. Chem.* **1993**, *33*, 345−350.

(19) Frisch, M. J.; Trucks, G. W.; Head-Gordon, M.; Gill, P. M. W.; Wong, M. W.; Foresman, J. B.; Jouhnson, B. G.; Schlegel, H. B.; Robb, M. A.; Replonge, E. S.; Gomperts, R.; Andres, J. L.; Raghavachari, K.; Binkley, J. S.; Gonzales, C.; Martin, R. L.; Fox, D. L.; Defrees, D. J.; Baker, J.; Stewart, J. J. P.; Pople, J. A., Gaussian, Inc.: Pittsburgh, PA, 1992.

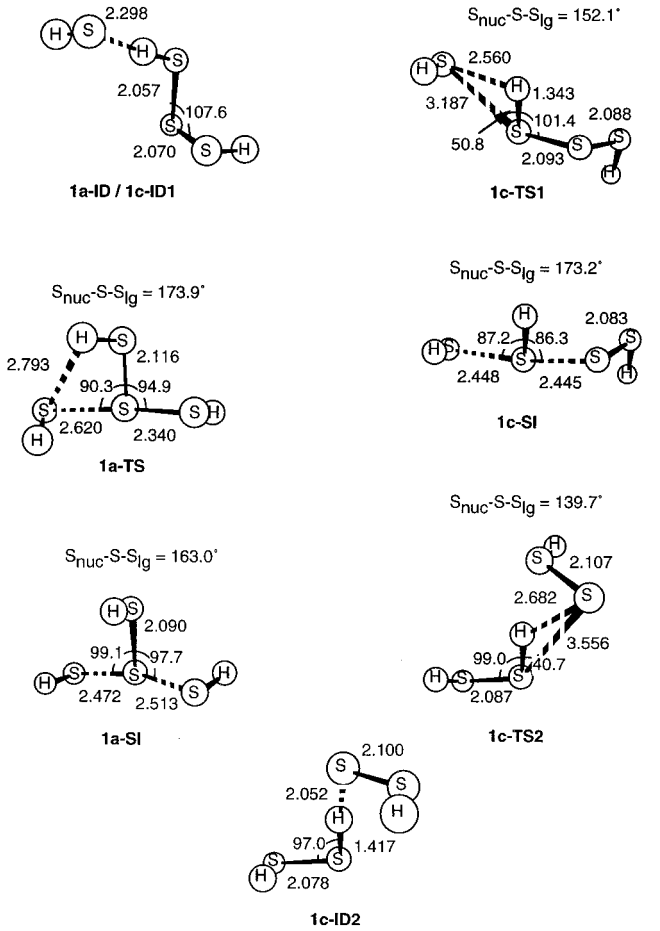

Figure 3. MP2/6-31+G* optimized geometries for the species in reaction 1.

thiolate at disulfides, we found that the nature of the reaction surface is sensitive to the inclusion of electronic correlation.[17] At the HF level, the reaction surface is a double well having one transition state (TS). However, at MP2 the surface has three wells, with a stable intermediate. This addition−elimination surface was confirmed at higher computational levels (MP4 and CCSD(T)). We were concerned that the same sensitivity to electron correlation would exist with the systems at study here.

At the HF/6-31G* level, the generalized reaction surface for the three reactions is given in Figure 2. This is the expected double-well potential for a classical gas-phase S_N2 surface.[21,22] Starting from isolated reactants, an ion−dipole complex forms (designated with the name **ID**). The reaction then continues through a single transition state (designated by **TS**) to an exit ion−dipole complex and then on to products. The relative energies of these critical points are listed in Table 1. For both reactions 1a and 1c, the TS has the expected backside attack of the nucleophile (Figure 1). The $S_{nuc}-S-S_{lg}$ angle is nearly linear and the breaking/forming S−S distances are similar. Similar double-well potentials were obtained for reactions 2 and 3 at HF/6-31+G* and their energies are given in Table 1.

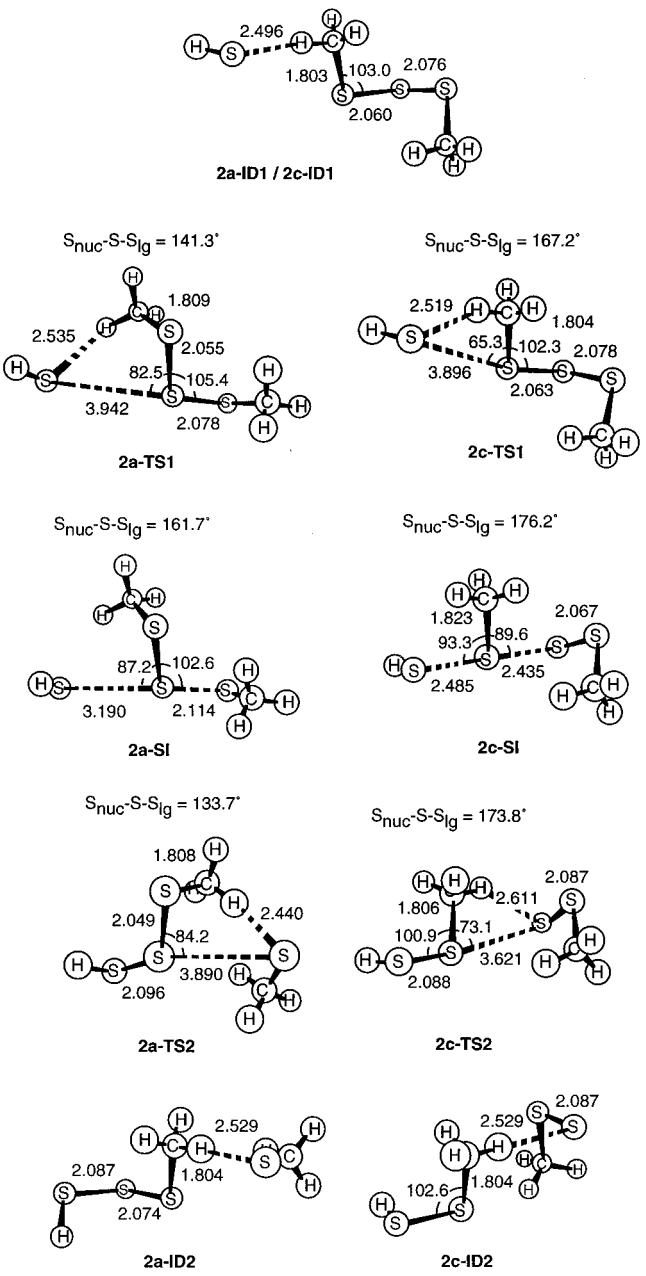

Figure 4. MP2/6-31+G* optimized geometries for the species in reaction 2.

As anticipated, the topology of the reaction surface changed dramatically upon inclusion of electron correlation at the MP2 level. This surface is shown in Figure 6. The HF TS changes little in structure upon optimization at MP2; however, it is a local minimum (no imaginary frequencies) at MP2 (designated by **SI**). A TS is found connecting the entry ion−dipole with this stable intermediate and a second TS connects the intermediate with the exit ion−dipole complex. The TSs are confirmed using the MP2 analytical frequency analysis. This triple-well potential persists at the MP4 level, where in fact the stable intermediate lies in a slightly deeper well (Table 2). These results are completely consistent with our previous study[17] and therefore we will discuss next only the MP2 and MP4 calculations for reactions 1−3.

Geometries. We will first examine nucleophilic attack at the center sulfur. The structures for reaction **1a** are drawn in Figure 3. The thiolate nucleophile interacts with the hydrogen on the trisulfide forming the complex **1a-ID**. From here the reaction proceeds through **1a-TS** which has one imaginary

(20) Frisch, M. J.; Trucks, G. W.; Schlegel, H. B.; Gill, P. M. W.; Johnson, B. G.; Robb, M. A.; Cheeseman, J. R.; Keith, T.; Petersson, G. A.; Montgomery, J. A.; Raghavachari, K.; Al-Laham, M. A.; Zakrzewski, V. G.; Ortiz, J. V.; Foresman, J. B.; Cioslowski, J.; Stefanov, B. B.; Nanayakkara, A.; Challacombe, M.; Peng, C. Y.; Ayala, P. Y.; Chen, W.; Wong, M. W.; Andres, J. L.; Reploge, E. S.; Gomperts, R.; Martin, R. L.; Fox, D. L.; Binkley, J. S.; Defrees, D. J.; Baker, J.; Stewart, J. J. P.; Head-Gordon, M.; Gonzales, C.; Pople, J. A., Gaussian, Inc.: Pittsburgh, PA, 1995.

(21) Brauman, J. I.; Olmstead, W. N.; Lieder, C. A. *J. Am. Chem. Soc.* **1974**, *96*, 4030−4031.

(22) Olmstead, W. N.; Brauman, J. I. *J. Am. Chem. Soc.* **1977**, *99*, 4219−4278.

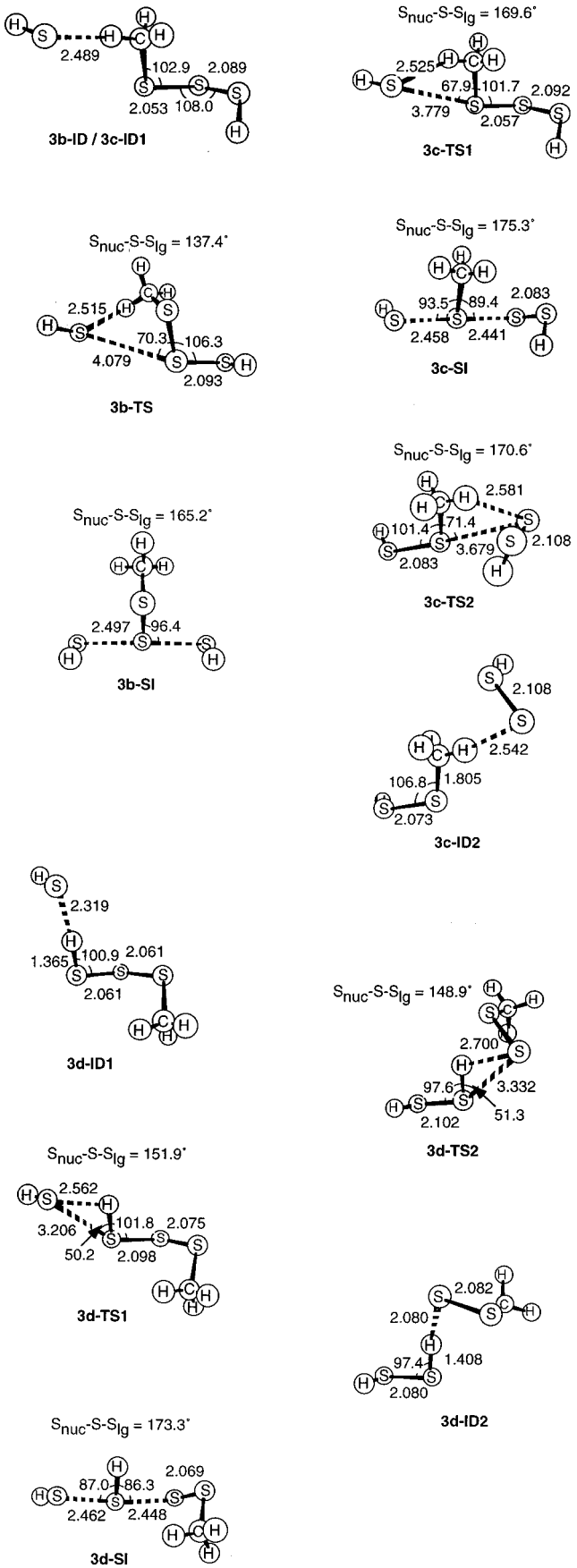

Figure 5. MP2/6-31+G* optimized geometries for the species in reaction 3.

frequency corresponding to the nucleophile moving away from the complexed H toward the central S. The important geometrical parameters are the forming $S_{nuc}-S$ bond distance of 2.620 Å, the breaking $S-S_{1g}$ bond distance of 2.340 Å, and the $S_{nuc}-S-S_{1g}$ angle of 173.9°. The TS then collapses to the intermediate, **1a-SI**, which is geometrically not very different from **1a-TS**. The small changes result in the forming and breaking S−S bonds being more equivalent, 2.472 and 2.513 Å, and the $S_{nuc}-S-S_{1g}$ angle is 163.0°, having the approaching and leaving group bending slightly more away from the group on the center sulfur. Since this reaction is an identity reaction, from **1a-SI** the reaction proceeds through **1a-TS** and **1a-ID** and on to the products.[23] MP2 optimization of **1a-ID** led to proton transfer to the nucleophile and so we report only single-point calculations using the HF structure. This problem has been observed in the reactions of disulfides when the nucleophile is a stronger base than the conjugate base of the disulfide.[17,24]

Analogous to **1a** is **3a** since this reaction also requires the formation of an ion−dipole complex to the hydrogen attached to a terminal sulfur of the trisulfide before attacking the center sulfur. Unfortunately, difficulties arose when trying to locate

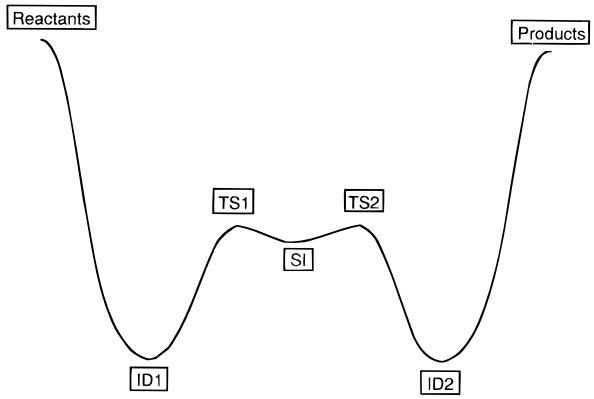

Figure 6. Representative reaction surface for the substitution reaction calculated at MP2.

Table 1. Relative Energies (kcal mol^{-1}) for Reactions **1a**−**3d** at HF/6-31+G* + ZPE[a]

reaction	reactants	ID1	TS	ID2	products
1a	0.0	−11.23	6.94	−11.23	0.0
1c	0.0	−11.23	−3.06	−14.74	−5.41
2a	0.0	−6.43	14.21	4.63	11.84
2c	0.0	−6.43	5.55	−8.68	−2.21
3a	0.0	−9.89	14.29	−0.42	12.02
3b	0.0	−7.08	7.17	−7.08	0.0
3c	0.0	−7.08	3.84	−11.05	−4.71
3d	0.0	−9.89	−1.22	−12.22	−2.73

[a] ZPE scaled by 0.9135.[18]

Table 2. Relative Energies (kcal mol^{-1}) for Reactions **1a**−**3d**[a]

reaction	reactants	**ID1**	**TS1**	**SI**	**TS2**	**ID2**	products
1a	0.0	−16.45[b]	−9.64	−10.28	−9.64	−16.45	0.0
	0.0	*−16.17*[c]	*−10.74*	*−11.51*	*−10.74*	*−16.17*	*0.0*
1c	0.0	−16.45[b]	−12.65	−15.09	−13.24	−17.68	−1.55
	0.0	*−16.17*[c]	*−12.95*	*−15.85*	*−13.12*	*−17.78*	*−1.43*
2a	0.0	−9.75	−6.87	−7.09	3.26	1.21	12.83
2c	0.0	−9.75	−9.68	−10.28	−8.96	−9.35	0.97
3b	0.0	−10.24	−7.65	−10.89	−7.65	−10.24	0.0
	0.0	*−10.66*	*−8.59*	*−12.31*	*−8.59*	*−10.66*	*0.0*
3c	0.0	−10.24	−10.10	−10.85	−9.74	−10.06	−0.27
	0.0	*−10.66*	*−10.79*	*−12.39*	*−10.52*	*−10.46*	*−0.07*
3d	0.0	−15.52[b]	−11.93	−14.39	−12.70	−16.41	−0.11
	0.0	*−15.26*[c]	*−12.35*	*−15.37*	*−13.29*	*−16.96*	*−0.38*

[a] MP2/6-31+G* + ZPE (scaled by 0.9646) energies are in normal type and MP4SDTQ/6-311+G**//MP2/6-31+G* + ZPE (scaled by 0.9646) energies are in italics. [b] MP2/6-31+G*//HF/6-31+G* + ZPE/HF (scaled by 0.9135). [c] MP4SDTQ/6-311+G**//HF/6-31+G* + ZPE/HF (scaled by 0.9135).

some of the structures for **3a**. We were not able to locate **3a-ID1**, **3a-TS1**, or **3a-SI** at MP2. Attempts to find these resulted in the hydrogen from the terminal sulfur of the trisulfide transferring to the nucleophile. Apparently, the CH_3SSSH is acidic enough to make a deprotonation reaction competitive with the substitution reaction. Therefore, we report no substitution reaction for **3a**.

Attack at the center sulfur in CH_3SSSCH_3, **2a**, is seen in Figure 4. The weakly hydrogen-bonded **2a-ID1** forms, having a slightly longer $S_{nuc}\cdots H$ distance than in **1a-ID** since the donor hydrogen is bonded to carbon instead of to sulfur. The first TS, **2a-TS1**, has a long $S_{nuc}\cdots S$ bond (3.942 Å), and only a minimally displaced leaving group. The angle of nucelophilic attack, relative to the leaving group is much smaller here in **2a-TS1** than in **1a-TS**, 141.3° compared to 173.9°. The intermediate next formed, **2a-SI**, shows a rather long $S_{nuc}\cdots S$ distance of 3.190 Å and a slightly elongated $S\cdots S_{1g}$ distance of 2.114 Å, which is a reflection of the nucleophile being a weaker base than the leaving group. The $S_{nuc}-S-S_{1g}$ angle has opened up to 161.7°. The second TS, **2a-TS2**, closely resembles **2a-TS1** in its geometric parameters, a long $S\cdots S_{1g}$ distance and a $S_{nuc}-S-S_{1g}$ angle of 133.7°. The second complex formed, **2a-ID2**, is comparable to **2a-ID1**.

The final reaction where attack is at the center sulfur is **3b**. These structures are drawn in Figure 5. This is an identity reaction, resulting in only one structure for the two IDs and one structure for the two TSs. All of the critical points for this reaction are consistent with the analogous reaction **2a**. The only difference between the two reactions is that in **3b**, the leaving group is HS^-, which gives a symmetrical SI (C_s symmetry), **3b-SI**, with $S\cdots S$ distances of 2.497 Å and the $S_{nuc}-S-S_{1g}$ angle is 165.2°.

Turning now to attack of a terminal sulfur, our results also indicate an addition−elimination path. The prototype reaction **1c** (Figure 3) initially forms **1c-ID1**, which is identical to **1a-ID**. The first TS, **1c-TS1**, results in an $S_{nuc}\cdots S$ distance of 3.187 Å, longer than for attack at the center sulfur in **1a-TS**. The thiosulfenate leaving group is affected little by the presence of the nucleophile in **1c-TS1**. The $S_{nuc}-S-S_{1g}$ angle is 152.1°, similar to what we saw in the TSs for attack at a disulfide.[17] The intermediate, **1c-SI**, has almost identical $S\cdots S$ distances, about 2.445 Å, and the angle between the nucleophile and leaving group opens up to 173.2°. The second TS, **1c-TS2**, resembles the products in that the leaving group is 3.556 Å away from the sulfur it was previously bonded to, and has a small $S_{1g}-S-S_{nuc}$ angle of 139.7°. Both sulfurs of the thiosulfenate leaving group interact with the hydrogen of the new HSSH molecule, a characteristic also seen in **1c-ID2**.

Analogous to **1c** is **3d**, shown in Figure 5. The structures for **3d** are very similar to those found for reaction **1c**. The methyl substituent is at the opposite end of the trisulfide chain from where attack occurs and, therefore, causes little effect.

Reactions **2c** and **3c** involve attack at a terminal sulfur possessing a methyl group, Figure 4 and 5. The structures for **3c** are analogous with those for **2c**, therefore only **2c** will be discussed. In **2c**, the nucleophile forms a weaker ion−dipole complex, suggested by the longer $S_{nuc}\cdots H$ distance of 2.496 Å in **2c-ID1** compared to the 2.298 Å distance in **1c-ID1**. This difference is mainly due to the complexed hydrogen being a methyl hydrogen versus a thiol hydrogen, where the latter is more acidic. Due to the presence of the methyl group, the $S_{nuc}\cdots S$ distance in the first TS, **2c-TS1**, is 0.709 Å longer than that in **1c-TS1**, where the terminal sulfur carries only a hydrogen. In addition, the $S_{nuc}-S-S_{1g}$ angle is 167.2° in **2c-TS1**, more than 15° larger than those in TSs of reactions **1c** or **3d**. Formation of the stable intermediate, **2c-SI**, requires a shortening of the $S_{nuc}\cdots S$ distance to 2.485 Å, a lengthening of the $S\cdots S_{1g}$ distance to 2.435 Å, and a widening of the $S_{nuc}-S-S_{1g}$ angle to 176.2°. Completing the reaction, **2c-TS2** closely mimics **2c-TS1**, having a long $S\cdots S$ distance of 3.621 Å, and a slightly less than linear arrangement for the $S_{nuc}-S-S_{1g}$ angle. Once again, the two sulfurs of the thiosulfenate of **2c-TS2** are electrostatically attracted to the nearest hydrogens, a feature also seen in **2c-ID2**.

Energies. The relative energies for all species in the reactions at MP2/6-31+G* + ZPE and at MP4SDTQ/6-311+G**//MP2/6-31+G* + ZPE are listed in Table 2.

The MP2 energies clearly show that the reaction coordinate for each of the reactions has three wells. A representative reaction coordinate is seen in Figure 6. The ion−dipole complexes lie in a deep well (about 10 to 17 kcal mol^{-1} more stable than the reactants). The stable intermediates lie in a much shallower well, ranging from 0.64 kcal mol^{-1} in reaction **1a** to 3.24 kcal mol^{-1} in reaction **3b**.

Since the shape of the potential energy surface changes from double-well at HF to triple-well at MP2, the larger MP4STDQ/6-311+G** single-point energy calculations were performed to assure that the MP2 surface is reasonable. For reactions 1 and 3, these larger calculations indicate that the MP2 **SI** does lie below **TS1** and **TS2**. In fact, the intermediates lie in a deeper well at MP4 than at MP2. The well depth increases by 0.13 kcal mol^{-1} for reaction **1a** to 0.85 kcal mol^{-1} for reaction **3c**.

The depth of the well where the **SI** lies varies by only a few kcal mol^{-1} in the three sets of reactions studied. The **1a** surface is pretty flat, with **1a-SI** only 0.64 kcal mol^{-1} lower in energy than **1a-TS1**. In **1c**, where attack is at the terminal sulfur, the well depth is 2.44 kcal mol^{-1} relative to **1c-TS1** (only 1.85 kcal mol^{-1} relative to **1c-TS2**). This region becomes even flatter if methyl groups are present, as **2a-SI** and **2c-SI** lie in very shallow wells (0.22 or 0.60 kcal mol^{-1}, respectively). The last set of reactions shows more of a variation; the well depth is 3.24 kcal mol^{-1} for **3b-SI**, about 1 kcal mol^{-1} for **3b-SI**, and 1.69 kcal mol^{-1} (2.46 relative to **3d-TS1**) for **3d-SI**.

There is distinct kinetic preference for attack at the terminal sulfur. For reaction 1, the activation energy for attack at the terminal sulfur **1c-TS1** is 3.01 kcal mol^{-1} lower than attack at the central sulfur **1a-TS1** (reduced to 2.21 kcal mol^{-1} at MP4). The preference for terminal attack is 2.81 kcal mol^{-1} for reaction 2. For reaction 3, the lowest TS is for attack at the hydrogen sulfur. Attack at the other terminal sulfur is 1.83 kcal mol^{-1} larger (1.56 kcal mol^{-1} at MP4), while the TS for attack at the central sulfur (reaction 3b) is 4.28 kcal mol^{-1} higher than in reaction 3d (3.76 kcal mol^{-1} at MP4).

Reaction energies for **1a-3d** are in the last column of Table 2. Comparison of these clearly shows that formation of the disulfide products from attack at the terminal sulfurs is more exothermic than for attack at the center sulfur. Reactions **1a** and **1c** show a preference of 1.5 kcal mol^{-1}, whereas there is almost a 12 kcal mol^{-1} preference in reaction 2. For reaction 3, terminal attack is favored by less than 0.5 kcal mol^{-1}.

Discussion

The mechanism for nucleophilic substitution at both the central and terminal sulfurs in trisulfides is addition−elimination

(23) There is at least one other path for reaction 1. Due to the symmetry of the system, the forward and backward paths are not identical. Another pathway goes through a SI that has C_s symmetry. This SI lies 0.19 kcal mol^{-1} above **1a-SI**. The path shown here is the lowest energy pathway. These alternative paths are discussed in more detail in ref 17.

(24) Grabowski, J. J.; Zhang, L. *J. Am. Chem. Soc.* **1989**, *111*, 1193−1203.

Table 3. NPA Charges on S in Trisulfides

molecule	$q(S_1)$	$q(S_2)$	$q(S_3)$
HS_2S_1SH	−0.04	−0.12	
$HS_2S_1S_3Me$	−0.04	−0.13	+0.11
MeS_2S_1SMe	−0.05	+0.09	

in the gas phase at MP2/6-31+G*. Starting from reactants (thiolate and disulfide), an ion−dipole complex forms, originating from a hydrogen bond between the sulfur anion and a hydrogen donated by the terminal sulfur or methyl group of the disulfide. Next, the thiolate swings toward the reacting sulfur, passing through a TS and forming a stable intermediate that has a hypercoordinate sulfur. Continuing on, the leaving group begins to dissociate, passing through a TS on its way to form an exit channel ion−dipole complex, before dissociating to products. This is completely analogous to the mechanism for nucleophilic substitution of disulfides.[17]

As found in our study of the disulfides, the mechanism for substitution of trisulfides is sensitive to electron correlation. The HF surface indicates an S_N2 mechanism while the MP2 surface is indicative of an addition−elimination mechanism. The MP4SDTQ/6-311+G**//MP2/6-31+G* energy calculations for the smaller systems (**1a**, **1c**, and **3a**−**3d**) fully support the MP2 reaction coordinate. In general, the MP4 calculations lower the energies of the TSs and SIs relative to the reactants for all paths. More important is the fact that the SIs are stabilized more than the TSs for all of the reactions, making the well that each SI occupies deeper.

Both the MP2 and MP4 energies indicate that nucleophilic attack at the terminal sulfur for all of the reactions is thermodynamically favored over attack at the central sulfur, which is a reflection of the thiosulfenate being a better leaving group than the thiolate. Furthermore, attack at the terminal sulfur is kinetically favored by about 2−5 kcal mol^{-1} for all of the reactions.

What is the origin of the preference for nucleophilic attack at the terminal position? A first approach might be to examine the charge distribution in the trisulfide moieties. Natural populations[25,26] for the sulfur atoms in the trisulfides are listed in Table 3. In dihydrogen trisulfide, all sulfurs carry net negative charge, with the terminal atoms slightly more negatively charged than the central sulfur. The charges suggest that nucleophilic attack will be unfavorable (the sulfur atoms carry negative charge) with a preference for attack at the central sulfur, which does not correspond with the calculated energies. For the methyl and dimethyl trisulfides, the terminal sulfur with the methyl substituent is slightly positively charged while the central sulfur carries net negative charge. While the central atom is thus predicted to be less susceptible to nucleophilic attack, NPA charge analysis suggests that reaction **3c** should be more favorable than reaction **3d**, which is not the case. Charge analysis sheds no light on this subject.

The simplest answer is that the terminal sulfur is less sterically crowded than the central sulfur. The central sulfur is blocked by the two large SR substituents. The terminal sulfur has either a hydrogen or methyl as one of its substituents and is therefore more accessible to the nucleophile.

Sterics alone, however, do not fully account for the selectivity. The hydrogen bonding in the ID preorganizes the system to a great extent for attack of the nucleophile at the terminal sulfur. This leads to substantially earlier TSs for attack at the terminal sulfur. In reaction 1, the nucleophilic S moves 0.47 Å closer to the terminal sulfur in going from **1a-ID** to **1c-TS1** but 2.00 Å in going from **1a-ID** to **1a-TS**. For reaction 2, the analogous distances are 0.43 Å in reaching **2c-TS1** and 2.35 Å to reach **2a-TS1**. Similar distances are found for reaction 3: 0.63 Å to **3c-TS1**, 2.25 Å to **3b-TS**, and 0.46 Å to **3d-TS1**.

The nucleophilic sulfur maintains an interaction with the hydrogen in all of the TSs. For **2a-TS1** and **3b-TS**, this means that the trisulfide chain must have a decidedly kinked backbone to allow the nucleophile to approach the central sulfur while still maintaining some interaction with the methyl hydrogen. The exit TSs also display a strong desire to maintain this favorable electrostatic interaction. When thiosulfenate is the leaving group, both sulfurs attempt to interact with the hydrogen, see **3c-TS2** and **3d-TS2**.

Another example of the effect of sterics and hydrogen bonding is the difference in activation energies for reactions **3c** and **3d**. The TS for reaction **3d** lies 1.83 kcal mol^{-1} (1.56 kcal mol^{-1} at MP4) lower than **3c-TS1**. Reaction **3d** involves the nucleophilic attack at the more accessible sulfur (H versus a methyl group) and also involves a stronger hydrogen bond through the sulfur hydrogen rather than a methyl hydrogen. (The substantially stronger hydrogen bond is apparent in the much lower energy of **3d-ID1** relative to **3c-ID1**.)

In the solution phase, this hydrogen bond between the nucleophile and disulfide will likely be unimportant. While we cannot "turn off" the hydrogen bonding in our calculations, there is little hydrogen bonding in the SIs, so their relative energies should better reflect a solution environment. (This analogy is likely to be very reasonable. In solution, the mechanism may change to S_N2 with the MP2 SI well approximating the S_N2 TS—recall the similarity in structure between the HF TS and MP2 SI.) For all three reactions, the SI coming from attack at the terminal sulfur is lower in energy than for attack at the central sulfur.

With the activation energy difference for attack at the terminal versus central sulfur less than 5 kcal mol^{-1}, we cannot exclude any pathway from being followed. Therefore, all modes of substitution are likely to occur, leading to a mixture of substitution products, with preference for products resulting from attack at the terminal sulfur. This is completely consistent with other reactions at trisulfides[6−8] and with the mixture of products Myers[10] observed during the reaction of calicheamicin with glutathione.

The three trisulfides we studied did not have an allyl substituent, as is present in calicheamicin, which might alter the relative energies of the TSs for the four different pathways. Therefore, we examined the reactions of methyl allyl trisulfide with thiolate, **4a**−**4d** (Scheme 3). Due to the size of these

Scheme 3

$$HS^- + CH_3SSSallyl \rightarrow HSSSCH_3 + allylS^- \quad \textbf{(4a)}$$

$$HS^- + CH_3SSSallyl \rightarrow HSSSallyl + CH_3S^- \quad \textbf{(4b)}$$

$$HS^- + CH_3SSSallyl \rightarrow HSSallyl + CH_3SS^- \quad \textbf{(4c)}$$

$$HS^- + CH_3SSSallyl \rightarrow HSSCH_3 + allylSS^- \quad \textbf{(4d)}$$

systems, we were only able to locate the TSs at the HF/6-31+G* level. Even though we have demonstrated that MP2 optimizations are needed to accurately define the mechanism, the HF/6-31+G* energies will provide a reasonable approximation of the relative energies. (This is based on the observation that

(25) Reed, A. E.; Weinstock, R. B.; Weinhold, F. *J. Chem. Phys.* **1985**, *83*, 735.

(26) Reed, A. E.; Weinhold, F. *J. Chem. Phys.* **1985**, *83*, 1736−1740.

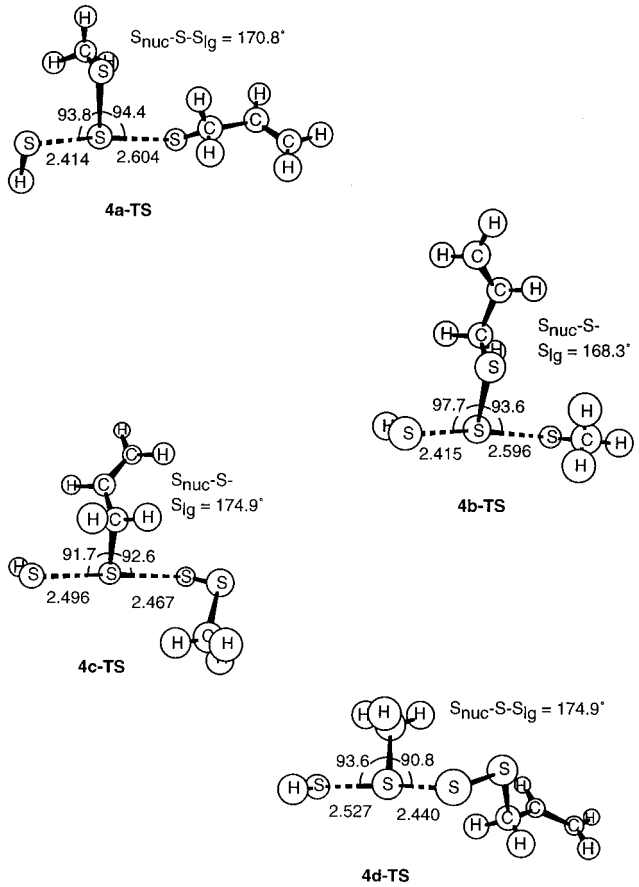

Figure 7. HF/6-31+G* optimized geometries of the TSs for reaction 4.

Table 4. Relative Energies (kcal mol^{-1}) of the TS for Reaction 4

structure	rel energy[a]
4a-TS	8.12
4b-TS	9.69
4c-TS	0.0
4d-TS	0.24

[a] HF/6-31+G* + ZPE (scaled by 0.9135).

the energetic ordering of the TSs for reactions 1−3 at HF/6-31+G* is consistent with the MP2 and MP4 ordering, see Tables 1 and 2.)

The structures of **4a-TS** through **4d-TS** are presented in Figure 7 and relative energies are listed in Table 4. These results for reaction 4 are consistent with what is found for reactions 1−3: attack at the terminal sulfur is kinetically favored (by at least 8 kcal mol^{-1} at HF) over attack at the central sulfur. The lowest energy TS, **4c-TS**, is for attack at the terminal allylic sulfur with formation of methylthiosulfenate and HSSallyl. Myers[10] also noted the preference for attack at the allylic sulfur of calicheamicin. The path that corresponds to the direct "trigger reaction" of calicheamicin, **4a-TS**, is in fact the third highest energy TS. Additional studies at higher computational levels on this system may alter these results, but the effect of correlation in energetic terms has not been more than a few kcal mol^{-1}. These HF/6-31+G* results clearly indicate a kinetic preference for nucleophilic substitution at the terminal sulfur. As Myers[10] has demonstrated, production of the desired allylS$^-$ results from multiple nucleophilic substitution steps and our results are in complete accord with his conclusions.

Conclusions

The three reactions studied indicate that nucleophilic substitution at both the central and terminal sulfurs of a trisulfide proceed via an addition−elimination mechanism. There is a kinetic preference for attack at a terminal sulfur over attack at the central sulfur of about 2 to 4 kcal mol^{-1}, but this preference is not enough to preclude attack at the central sulfur. The preference for attack at the terminal sulfur is largely due to the steric hindrance found around the central sulfur, along with a favorable hydrogen bonding interaction that best preorganizes the system for attack at the terminal position. There is also a slight thermodynamic preference for attack at the terminal sulfur due to thiosulfenate being a better leaving group than a thiolate anion.

Since the preference for attack at a terminal sulfur is not large, nucleophilic attack is likely to occur at all three sulfur atoms for the activation of calicheamicin. All four possible pathways will occur to some extent. The preference for terminal attack will lead to disulfide and thiosulfenate as the major products. Our HF results show that attack at the center sulfur of the calicheamicin mimic (methyl allyl trisulfide), displacing the allylic thiolate, is not the favored path. This is in close agreement with Myers' results concerning the kinetics of glutathione substitution on calichaemicin.[10] These results support the mechanistic findings of Myers[10] that the trigger mechanism for **1** is a multistep process; the most rapid displacements occur at the terminal sulfur resulting in disulfide products which then undergo a second substitution, yielding the appropriate precursor for internal Michael addition that begins the cascade events toward biological activation.

Acknowledgment is made to the National Science Foundation for support of this research.

JA9620090